




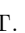











## Indications of a Cosmic Ray Source in the Perseus-Pisces Supercluster

THE TELESCOPE ARRAY COLLABORATION

R.U. ABBASI <sup>1</sup>, T. ABU-ZAYYAD <sup>1,2</sup>, M. ALLEN,<sup>2</sup> Y. ARAI,<sup>3</sup> R. ARIMURA,<sup>3</sup> E. BARCIKOWSKI,<sup>2</sup> J.W. BELZ,<sup>2</sup> D.R. BERGMAN,<sup>2</sup> S.A. BLAKE,<sup>2</sup> I. BUCKLAND,<sup>2</sup> R. CADY,<sup>2</sup> B.G. CHEON,<sup>4</sup> J. CHIBA,<sup>5</sup> M. CHIKAWA,<sup>6</sup> T. FUJII <sup>7</sup>, K. FUJISUE,<sup>6</sup> K. FUJITA,<sup>3</sup> R. FUJIWARA,<sup>3</sup> M. FUKUSHIMA,<sup>6</sup> R. FUKUSHIMA,<sup>3</sup> G. FURLICH,<sup>2</sup> N. GLOBUS,<sup>8,\*</sup> R. GONZALEZ,<sup>2</sup> W. HANLON <sup>2</sup>, M. HAYASHI,<sup>9</sup> N. HAYASHIDA,<sup>10</sup> K. HIBINO,<sup>10</sup> R. HIGUCHI,<sup>6</sup> K. HONDA,<sup>11</sup> D. IKEDA <sup>10</sup>, T. INADOMI,<sup>12</sup> N. INOUE,<sup>13</sup> T. ISHII,<sup>11</sup> H. ITO,<sup>8</sup> D. IVANOV <sup>2</sup>, H. IWAKURA,<sup>12</sup> A. IWASAKI,<sup>3</sup> H.M. JEONG,<sup>14</sup> S. JEONG,<sup>14</sup> C.C.H. JUI <sup>2</sup>, K. KADOTA,<sup>15</sup> F. KAKIMOTO,<sup>10</sup> O. KALASHEV,<sup>16</sup> K. KASAHARA <sup>17</sup>, S. KASAMI,<sup>18</sup> H. KAWAI,<sup>19</sup> S. KAWAKAMI,<sup>3</sup> S. KAWANA,<sup>13</sup> K. KAWATA,<sup>6</sup> I. KHARUK,<sup>16</sup> E. KIDO,<sup>8</sup> H.B. KIM,<sup>4</sup> J.H. KIM,<sup>2</sup> J.H. KIM <sup>2</sup>, M.H. KIM,<sup>14</sup> S.W. KIM,<sup>14</sup> Y. KIMURA,<sup>3</sup> S. KISHIGAMI,<sup>3</sup> Y. KUBOTA,<sup>12</sup> S. KURISU,<sup>12</sup> V. KUZMIN,<sup>16,†</sup> M. KUZNETSOV,<sup>20,16</sup> Y.J. KWON,<sup>21</sup> K.H. LEE,<sup>14</sup> B. LUBSANDORZHIEV,<sup>16</sup> J.P. LUNDQUIST,<sup>22,2</sup> K. MACHIDA,<sup>11</sup> H. MATSUMIYA,<sup>3</sup> T. MATSUYAMA,<sup>3</sup> J.N. MATTHEWS <sup>2</sup>, R. MAYTA,<sup>3</sup> M. MINAMINO,<sup>3</sup> K. MUKAI,<sup>11</sup> I. MYERS,<sup>2</sup> S. NAGATAKI,<sup>8</sup> K. NAKAI,<sup>3</sup> R. NAKAMURA,<sup>12</sup> T. NAKAMURA,<sup>23</sup> T. NAKAMURA,<sup>12</sup> Y. NAKAMURA,<sup>12</sup> A. NAKAZAWA,<sup>12</sup> E. NISHIO,<sup>18</sup> T. NONAKA,<sup>6</sup> H. ODA,<sup>3</sup> S. OGIO,<sup>24,3</sup> M. OHNISHI,<sup>6</sup> H. OHOKA,<sup>6</sup> Y. OKU,<sup>18</sup> T. OKUDA,<sup>25</sup> Y. OMURA,<sup>3</sup> M. ONO,<sup>8</sup> R. ONOGI,<sup>3</sup> A. OSHIMA,<sup>26</sup> S. OZAWA,<sup>27</sup> I.H. PARK,<sup>14</sup> M. POTTS <sup>2</sup>, M.S. PSIRKOV,<sup>16,28</sup> J. REMINGTON,<sup>2</sup> D.C. RODRIGUEZ,<sup>2</sup> G.I. RUBTSOV <sup>16</sup>, D. RYU,<sup>29</sup> H. SAGAWA,<sup>6</sup> R. SAHARA,<sup>3</sup> Y. SAITO,<sup>12</sup> N. SAKAKI,<sup>6</sup> T. SAKO,<sup>6</sup> N. SAKURAI,<sup>3</sup> K. SANO,<sup>12</sup> K. SATO,<sup>3</sup> T. SEKI,<sup>12</sup> K. SEKINO,<sup>6</sup> P.D. SHAH,<sup>2</sup> Y. SHIBASAKI,<sup>12</sup> F. SHIBATA,<sup>11</sup> N. SHIBATA,<sup>18</sup> T. SHIBATA,<sup>6</sup> H. SHIMODAIRA,<sup>6</sup> B.K. SHIN,<sup>29</sup> H.S. SHIN,<sup>6</sup> D. SHINTO,<sup>18</sup> J.D. SMITH,<sup>2</sup> P. SOKOLSKY,<sup>2</sup> N. SONE,<sup>12</sup> B.T. STOKES,<sup>2</sup> T.A. STROMAN,<sup>2</sup> Y. TAKAGI,<sup>3</sup> Y. TAKAHASHI,<sup>3</sup> M. TAKAMURA,<sup>5</sup> M. TAKEDA,<sup>6</sup> R. TAKEISHI,<sup>6</sup> A. TAKETA,<sup>30</sup> M. TAKITA,<sup>6</sup> Y. TAMEDA <sup>18</sup>, H. TANAKA,<sup>3</sup> K. TANAKA,<sup>31</sup> M. TANAKA,<sup>32</sup> Y. TANOUE,<sup>3</sup> S.B. THOMAS,<sup>2</sup> G.B. THOMSON,<sup>2</sup> P. TINYAKOV,<sup>20,16</sup> I. TKACHEV,<sup>16</sup> H. TOKUNO,<sup>33</sup> T. TOMIDA,<sup>12</sup> S. TROITSKY <sup>16</sup>, R. TSUDA,<sup>3</sup> Y. TSUNESADA <sup>24,3</sup>, Y. UCHIHORI,<sup>34</sup> S. UDO,<sup>10</sup> T. UEHAMA,<sup>12</sup> F. URBAN,<sup>35</sup> T. WONG,<sup>2</sup> M. YAMAMOTO,<sup>12</sup> K. YAMAZAKI,<sup>26</sup> J. YANG,<sup>36</sup> K. YASHIRO,<sup>5</sup> F. YOSHIDA,<sup>18</sup> Y. YOSHIOKA,<sup>12</sup> Y. ZHEZHER,<sup>6,16</sup> Z. ZUNDEL,<sup>2</sup>

<sup>1</sup>Department of Physics, Loyola University Chicago, Chicago, Illinois, USA

<sup>2</sup>High Energy Astrophysics Institute and Department of Physics and Astronomy, University of Utah, Salt Lake City, Utah, USA

<sup>3</sup>Graduate School of Science, Osaka City University, Osaka, Osaka, Japan

<sup>4</sup>Department of Physics and The Research Institute of Natural Science, Hanyang University, Seongdong-gu, Seoul, Korea

<sup>5</sup>Department of Physics, Tokyo University of Science, Noda, Chiba, Japan

<sup>6</sup>Institute for Cosmic Ray Research, University of Tokyo, Kashiwa, Chiba, Japan

<sup>7</sup>The Hakubi Center for Advanced Research and Graduate School of Science, Kyoto University, Kitashirakawa-Oiwakecho, Sakyo-ku, Kyoto, Japan

<sup>8</sup>Astrophysical Big Bang Laboratory, RIKEN, Wako, Saitama, Japan

<sup>9</sup>Information Engineering Graduate School of Science and Technology, Shinshu University, Nagano, Nagano, Japan

<sup>10</sup>Faculty of Engineering, Kanagawa University, Yokohama, Kanagawa, Japan

<sup>11</sup>Interdisciplinary Graduate School of Medicine and Engineering, University of Yamanashi, Kofu, Yamanashi, Japan

<sup>12</sup>Academic Assembly School of Science and Technology Institute of Engineering, Shinshu University, Nagano, Nagano, Japan

<sup>13</sup>The Graduate School of Science and Engineering, Saitama University, Saitama, Saitama, Japan

<sup>14</sup>Department of Physics, SungKyunKwan University, Jang-an-gu, Suwon, Korea

<sup>15</sup>Department of Physics, Tokyo City University, Setagaya-ku, Tokyo, Japan

<sup>16</sup>Institute for Nuclear Research of the Russian Academy of Sciences, Moscow, Russia

<sup>17</sup>Faculty of Systems Engineering and Science, Shibaura Institute of Technology, Minato-ku, Tokyo, Japan

<sup>18</sup>Department of Engineering Science, Faculty of Engineering, Osaka Electro-Communication University, Neyagawa-shi, Osaka, Japan

<sup>19</sup>Department of Physics, Chiba University, Chiba, Chiba, Japan

<sup>20</sup>Service de Physique Théorique, Université Libre de Bruxelles, Brussels, Belgium

<sup>21</sup>Department of Physics, Yonsei University, Seodaemun-gu, Seoul, Korea

<sup>22</sup>Center for Astrophysics and Cosmology, University of Nova Gorica, Nova Gorica, Slovenia

<sup>23</sup>Faculty of Science, Kochi University, Kochi, Kochi, Japan

<sup>24</sup>Nambu Yoichiro Institute of Theoretical and Experimental Physics, Osaka City University, Osaka, Osaka, Japan

Corresponding author: Jihyun Kim

jihyun@cosmic.utah.edu

<sup>25</sup>*Department of Physical Sciences, Ritsumeikan University, Kusatsu, Shiga, Japan*

<sup>26</sup>*College of Engineering, Chubu University, Kasugai, Aichi, Japan*

<sup>27</sup>*Quantum ICT Advanced Development Center, National Institute for Information and Communications Technology, Koganei, Tokyo, Japan*

<sup>28</sup>*Sternberg Astronomical Institute, Moscow M.V. Lomonosov State University, Moscow, Russia*

<sup>29</sup>*Department of Physics, School of Natural Sciences, Ulsan National Institute of Science and Technology, UNIST-gil, Ulsan, Korea*

<sup>30</sup>*Earthquake Research Institute, University of Tokyo, Bunkyo-ku, Tokyo, Japan*

<sup>31</sup>*Graduate School of Information Sciences, Hiroshima City University, Hiroshima, Hiroshima, Japan*

<sup>32</sup>*Institute of Particle and Nuclear Studies, KEK, Tsukuba, Ibaraki, Japan*

<sup>33</sup>*Graduate School of Science and Engineering, Tokyo Institute of Technology, Meguro, Tokyo, Japan*

<sup>34</sup>*Department of Research Planning and Promotion, Quantum Medical Science Directorate, National Institutes for Quantum and Radiological Science and Technology, Chiba, Chiba, Japan*

<sup>35</sup>*CEICO, Institute of Physics, Czech Academy of Sciences, Prague, Czech Republic*

<sup>36</sup>*Department of Physics and Institute for the Early Universe, Ewha Womans University, Seodaemun-gu, Seoul, Korea*

## ABSTRACT

The Telescope Array Collaboration has observed an excess of events with  $E \geq 10^{19.4}$  eV in the data which is centered at (RA, dec) = (19°, 35°). This is near the center of the Perseus-Pisces supercluster (PPSC). The PPSC is about 70 Mpc distant and is the closest supercluster in the Northern Hemisphere (other than the Virgo supercluster of which we are a part). A Li-Ma oversampling analysis with 20°-radius circles indicates an excess in the arrival direction of events with a local significance of about 4 standard deviations. The probability of having such excess close to the PPSC by chance is estimated to be 3.5 standard deviations. This result indicates that a cosmic ray source likely exists in that supercluster.

*Keywords:* Particle astrophysics (96), Ultra-high-energy cosmic radiation (1733), Cosmic rays (329), Cosmic ray astronomy (324), Large-scale structure of the universe (902), Cosmic ray sources (328)

## 1. INTRODUCTION

Ultrahigh energy cosmic rays (UHECR) are energetic particles originating from outer space, having energies greater than  $10^{18}$  eV, that impinge on the Earth's atmosphere. Their sources remain one of the most important questions to be answered. The main areas of UHECR study are their energy spectrum, mass composition, and searches for anisotropy, which are expected to shed light on the question of sources. The Telescope Array (TA) hotspot (Abbasi et al. 2014) which is about 20° in radius and centered at (146.7°, 43.2°) is one indication of anisotropy. Other previous signs are the Auger dipole (Aab et al. 2017), most of the evidence for which is in the southern hemisphere, and the Auger excess (Aab et al. 2015) near the location of Centaurus A, the closest active galactic nucleus. The nearby Virgo cluster, dominated by M87, does not appear as an excess in UHECR data.

The TA collaboration hotspot, reported in 2014 (Abbasi et al. 2014), was found in the arrival direction of UHECR events with energy greater than 57 EeV in the northern sky. In that publication, an oversampling analysis using the intermediate angular scale of 20°-radius circles was conducted for the first 5 years of data collected with the TA scintillator surface detector array. The maximum excess appeared at the position (146.7°, 43.2°) in equatorial coordinates with a Li-Ma significance of  $5.1\sigma$ . The probability of having such an excess by chance was estimated via Monte Carlo (MC) studies to be  $3.4\sigma$ . However, there are no known prominent sources aligned with the hotspot within the cosmic ray events' horizon. There have been correlation studies between the hotspot and possible sources (He et al. 2016; Kim et al. 2019); however, the source of the hotspot remains inconclusive. The hotspot persists in TA data with over  $3\sigma$  significance (Kim et al. 2021).

In the Northern Hemisphere, the next closest component of the local large-scale structure is the Perseus-Pisces supercluster (PPSC). It stretches across the sky from the Perseus cluster to the Pegasus cluster and con-

\* Presently at: University of California - Santa Cruz and Flatiron Institute, Simons Foundation

† Deceased

tains about 16 galactic clusters and groups containing tens of thousands of galaxies.

In this paper, we report a new excess of events at slightly lower energies than the original hotspot. While studying the spectrum mismatch above  $10^{19.5}$  eV seen in the TA and Auger data (Abbasi et al. 2021a), we made sky maps of events for energy ranges,  $E \geq 10^{19.4}$  eV,  $E \geq 10^{19.5}$  eV, and  $E \geq 10^{19.6}$  eV. The maximum Li-Ma significance appeared at the location of the PPSC for each energy range. We now present these three data sets.

The structure of this paper is as follows. In Section 2 we describe the TA experiment and the data used in this study. Section 3 has three parts. First, we present the Li-Ma oversampling analysis using  $20^\circ$ -radius circles to determine the significance of the excess of events in arrival directions. Then we show sky maps made with the representative elements of the PPSC. Finally, we describe the MC simulation used to estimate the chance probability of having an excess close by the prominent local large-scale structures. In Section 4 we summarize our findings.

## 2. TA EXPERIMENT AND THE DATA

The TA is the largest observatory for UHECRs in the Northern Hemisphere. The observatory is approximately 1400 m above sea level, and it is centered at  $39.3^\circ\text{N}$  and  $112.9^\circ\text{W}$ , in the west desert of Utah, USA. It consists of a surface detector (SD) array and three fluorescence detector (FD) stations viewing the sky over the array. It is designed for observing extensive air showers induced by UHECRs using a hybrid technique.

The SD array consists of 507 plastic scintillation detectors deployed on a square grid with 1.2 km spacing, covering a total area of  $\sim 700$  km<sup>2</sup> (Abu-Zayyad et al. 2012). They measure the shower footprint and lateral distribution at the Earth's surface. Three FD stations, instrumented with 38 telescopes, are situated at the apices of a triangle with each station having a field of view overlooking the area of the SD array (Tokuno et al. 2012). The FDs are suitable for measuring the longitudinal shower development of events to estimate the mass of the primary particle; however, their data are limited to  $\sim 10\%$  duty cycle since they operate only on moonless nights. In this study, we focus on the data recorded by the SD array to take full advantage of its high duty cycle (greater than 95%).

For this work, we used the data collected between May 11 of 2008 and May 10 of 2019—a data-taking period of 11 years. The event selection criteria that apply to the data are as follows:

1. Energy  $\geq 10^{19.4}$  eV,

2. Zenith angle of arrival direction  $< 55^\circ$ ,

3. At least five SDs triggered,

4. Shower geometry and lateral distribution function fit  $\chi^2/\text{dof} < 4$ ,

5. Reconstructed pointing direction error  $< 5^\circ$ ,

6. The fractional uncertainty of the energy estimator  $S_{800} < 25\%$ ,

7. The largest signal counter is surrounded by four working counters: there must be at least one working counter to the left, right, down, up on the grid of counter with the largest signal. These counters do not have to be immediate neighbors of the largest signal counter.

These are our standard selection criteria that have been used previously for anisotropy studies. The energy of reconstructed events is determined by the SD  $S_{800}$  which is then renormalized by  $1/1.27$  as previously determined to match the SD scale to the calorimetrically determined FD energy scale (Abu-Zayyad et al. 2013). A total of 864 events meet these selection criteria. The energy and angular resolution of events are from 10% to 20% and  $1.0^\circ$  to  $1.5^\circ$ , respectively (Abbasi et al. 2018).

## 3. LI-MA OVERSAMPLING ANALYSIS

In conducting the spectrum study where this work originated (Abbasi et al. 2021a), part of our investigation was whether the hotspot extends down into lower declinations at slightly lower energies. Therefore, we adopted  $20^\circ$  angular windows for oversampling to be consistent with the original hotspot analysis method (Abbasi et al. 2014). As a result, we found new excesses of events in the distribution of arrival directions.

The TA observes from  $90^\circ$  to  $-15.7^\circ$  in declination and  $0^\circ$  to  $360^\circ$  in right ascension. To estimate the background event rate,  $10^5$  events were generated within that field of view, assuming an isotropic flux and taking into account the geometrical exposure of the SD. The statistical significance of the excess of the data was compared to the isotropic events at each grid point, using  $0.1^\circ \times 0.1^\circ$  grid spacing. The significance was calculated utilizing the Li-Ma method (Li & Ma 1983):

$$S_{LM} = \sqrt{2} \left[ N_{\text{on}} \ln \left( \frac{(1+\alpha)N_{\text{on}}}{\alpha(N_{\text{on}}+N_{\text{off}})} \right) + N_{\text{off}} \ln \left( \frac{(1+\alpha)N_{\text{off}}}{N_{\text{on}}+N_{\text{off}}} \right) \right]^{1/2}, \quad (1)$$

where  $\alpha = N_{\text{sim,circle}}/(N_{\text{sim,total}} - N_{\text{sim,circle}})$ . Here,  $N_{\text{sim,total}}$  is the total number of isotropic background events we generated,  $N_{\text{sim,total}} = 10^5$ ,  $N_{\text{sim,circle}}$  means the number of isotropic events inside the  $20^\circ$ -radius circle at each grid point,  $N_{\text{on}}$  represents the number of observed events inside the circle at the same grid point, and  $N_{\text{off}} = N_{\text{data,total}} - N_{\text{on}}$ , where  $N_{\text{data,total}}$  is the total

number of data in each data set. The number of background events inside the  $20^\circ$ -radius circle is estimated by the exposure ratio  $\alpha$  and the data,  $N_{\text{bg}} = \alpha N_{\text{off}}$ .

When compared to the isotropic background events, new Li-Ma significance results are calculated for each energy cut and are summarized as follows. For  $E \geq 10^{19.4}$  eV, the maximum Li-Ma significance appears at  $(17.4^\circ, 36.0^\circ)$  with  $4.4\sigma$ . There are 85 out of 864 observed events within the central  $20^\circ$ -radius circle oversampling, whereas 49.5 events are expected as background from the isotropic assumption. For  $E \geq 10^{19.5}$  eV, the maximum Li-Ma significance appears at  $(19.0^\circ, 35.1^\circ)$  with  $4.2\sigma$ . There are 59 out of 558 observed events within the central  $20^\circ$ -radius circle oversampling, whereas 31.5 events are expected as background from the isotropic assumption. For  $E \geq 10^{19.6}$  eV, the maximum Li-Ma significance appears at  $(19.7^\circ, 34.6^\circ)$  with  $4.0\sigma$ . There are 39 out of 335 observed events within the central  $20^\circ$ -radius circle oversampling, whereas 18.6 events are expected as background from the isotropic assumption.

Figure 1 shows the excesses of events with  $E \geq 10^{19.4}$  eV,  $10^{19.5}$  eV,  $10^{19.6}$  eV, and 57 EeV, respectively. The color scheme represents the Li-Ma significance explained above. On each map, we indicated the position of maximum Li-Ma significance, excess with respect to isotropy, with a black diamond. For the three lower energies, the new excesses of events appear consistently in the direction to the left of the center in the sky maps in Figure 1. For the highest energy set, with  $E \geq 57$  EeV, the maximum significance of the sky map shifts to the region in the figure which is the hotspot reported in 2014 (Abbasi et al. 2014). A smaller excess remains visible in the direction of the maximum at lower energies.

Next, we investigated the time variation of the excess by dividing the data into two time periods. As an example, the sky map is shown in Figure 2 for the data set with  $E \geq 10^{19.5}$  eV. The map is shown for the first 5-years of data adjacent to the map for the last 6-years of data. There is no apparent difference in the excess between the maps of the two data sets. Both maps have similar local significances, around  $3\sigma$ , toward the new excess region. The distributions of the other two energy cuts demonstrate similar local significances. This is indicative of a steady state excess in this region.

The new excess of events appears in the region of the Perseus-Pisces supercluster (PPSC), which is one of the notable structures within TA's field of view. This is a possible source for the observed excess. The PPSC is the closest supercluster other than the local supercluster which we reside in. It is known that the PPSC has a gigantic filamentary structure, stretching for over

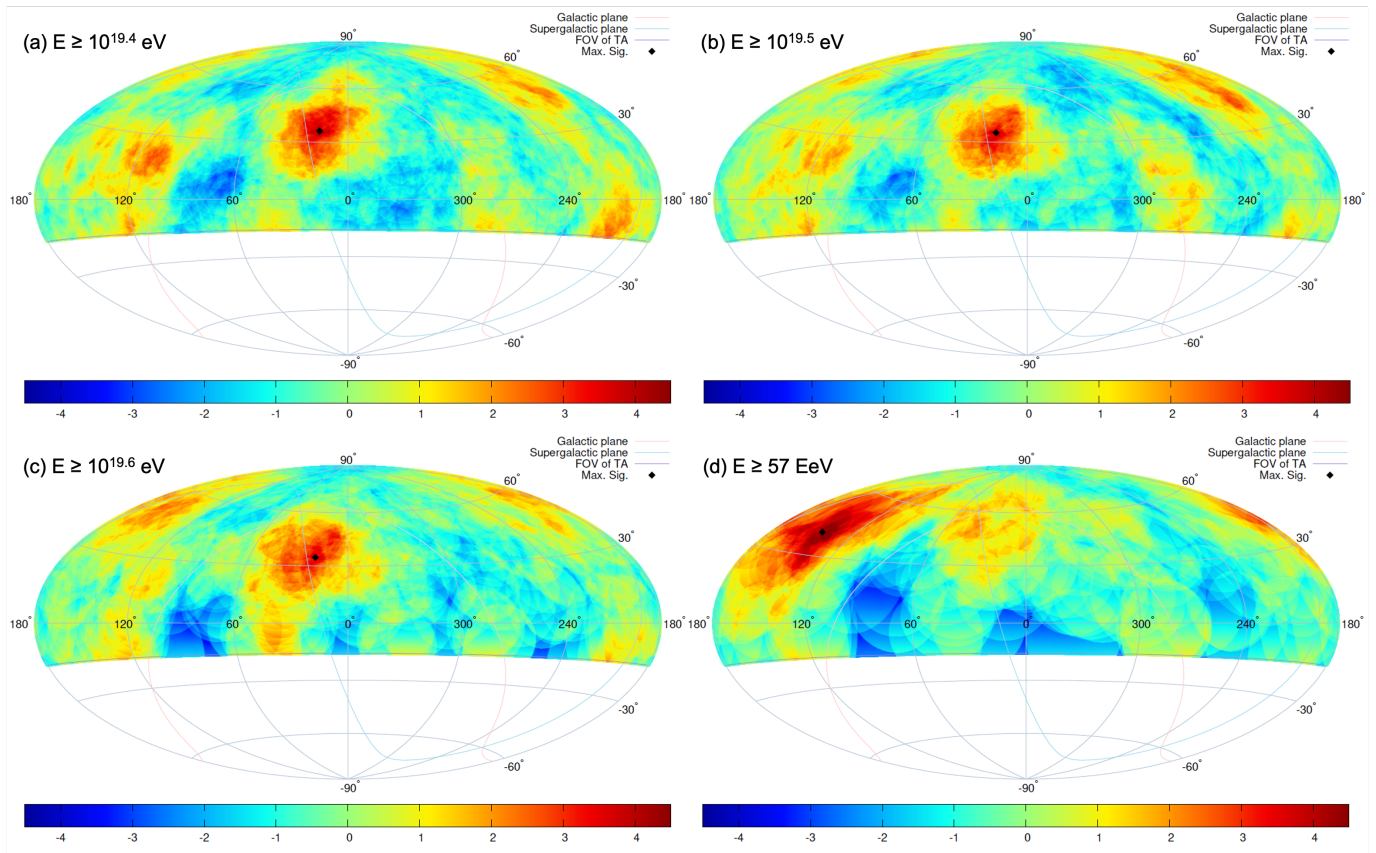
300 Mpc/h (Batuski & Burns 1985). According to Haynes and Giovanelli (Haynes & Giovanelli 1986), the major portion of the foreground between the Earth and the PPSC as well as the space beyond the PPSC in the same direction, are nearly empty. Courtois *et al.* provide density contour maps after making corrections for catalog incompleteness (Courtois et al. 2013). Figure 8 in that paper shows the PPSC appears as an elongated structure of galaxies. No prominent structures between the Earth and the PPSC, or beyond the PPSC, are seen in the direction of the new excess of events in that figure. If the new excess of events in arrival direction distribution has an astrophysical origin, the PPSC could be responsible for it.

Figure 3 shows the new excess in a series of expanded sky maps with the PPSC overlaid upon it. The data has been plotted for the three energy cuts using the Li-Ma significances. To show the elements of the PPSC on the sky, we adopt the list that includes the major clusters of galaxies and the major groups of galaxies that comprise the PPSC in reference (PPSC 2021). These are marked with asterisks in the three maps. The excess is coincident with the overall distribution of the PPSC.

It is suggestive that the excess in the data falls on top of the PPSC. To quantify how often this happens by chance, we generate many isotropic MC event sets thrown according to the acceptance of the TA SD. Each MC set contains the same number of events as the data. We count as successes the number of MC sets where the maximum Li-Ma significance is at least as significant in the MC set as in the data and which occurs at least as close to the PPSC as the data.

We begin by defining the directional center of the PPSC using the mean values of the right ascensions and declinations of its representative elements. It is calculated to be  $(20.9^\circ, 27.9^\circ)$  in equatorial coordinates, which is indicated by the blue square in Figure 3. In addition, the center position of the excess, where the maximum Li-Ma significance is estimated, is represented by the cyan diamond in the figure. Next, we calculate the angular distances between the center of the PPSC and the positions of the maximum excesses—  $(17.4^\circ, 36.0^\circ)$ ,  $(19.0^\circ, 35.1^\circ)$ , and  $(19.7^\circ, 34.6^\circ)$  for each energy threshold. Their angular separation is  $8.6^\circ$  for  $10^{19.4}$  eV,  $7.4^\circ$  for  $10^{19.5}$  eV, and  $6.8^\circ$  for  $10^{19.6}$  eV.

The steps for performing the MC simulations are as follows. At each energy threshold,  $10^{19.4}$  eV,  $10^{19.5}$  eV, and  $10^{19.6}$  eV, we throw  $5 \times 10^5$  sets of MC trials with the same statistics as the data and perform a Li-Ma analysis of each trial, which gives us the maximum Li-Ma significance and its position. Then, we calculate the angle,  $\theta_{\text{mc}}$ , between the position that has the MC's maximum



**Figure 1.** Sky maps in equatorial coordinates using Hammer projections. The color scheme indicates the Li-Ma significance and shows the excess (red) or deficit (blue) of events compared to isotropy at each grid point. The positions of maximum excesses are marked with the black diamonds. An intermediate angular scale of  $20^\circ$ -radius circles was used for oversampling analysis for different energy thresholds. The energy cut for each map is (a)  $E \geq 10^{19.4}$  eV, (b)  $E \geq 10^{19.5}$  eV, (c)  $E \geq 10^{19.6}$  eV, and (d)  $E \geq 57$  EeV. For three lower energies, (a) to (c), a new excess of events is consistently observed in the same direction. When the energy cut is raised to  $E \geq 57$  EeV (d), the maximum significance moves to the previously observed hotspot, however, a smaller excess remains. Note that the right ascension of  $0^\circ$  is at the center of the sky map.

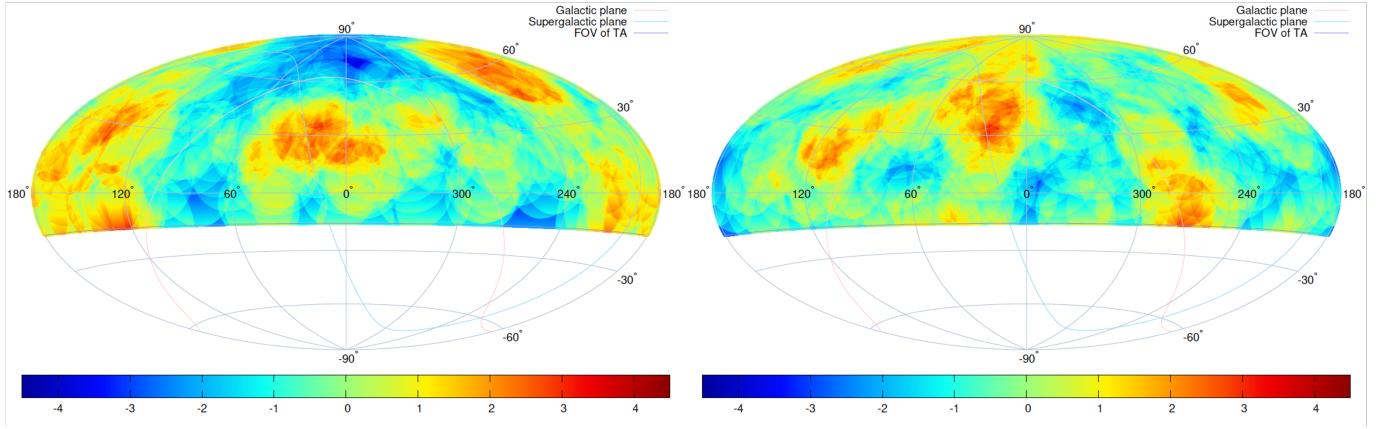
Li-Ma significance and the center of the PPSC. We count as successes those within angle  $\theta_{\text{obs}}$  of the PPSC with an equal or greater significance than the data with the PPSC: ( $S_{\text{mc}} \geq S_{\text{obs}}$ ) and ( $\theta_{\text{mc}} \leq \theta_{\text{obs}}$ ). By requiring the MC set to meet or exceed the conditions of the data, we estimate the probability of having an equal or greater excess coincident with the PPSC by chance. The chance probabilities of having an excess this significant overlapping the PPSC are estimated to be  $3.6\sigma$ ,  $3.6\sigma$ , and  $3.4\sigma$  for  $E \geq 10^{19.4}$  eV,  $E \geq 10^{19.5}$  eV, and  $E \geq 10^{19.6}$  eV, respectively.

We investigate the data further by taking into account the major objects in the local large-scale structure of the universe similar to the PPSC within the TA's field of view: the Virgo cluster (17 Mpc), Coma supercluster (90 Mpc), Leo supercluster (135 Mpc), and Hercules supercluster (135 Mpc). Their center positions are defined in the same manner as defining the PPSC center, which are marked with the black squares in Figure 4.

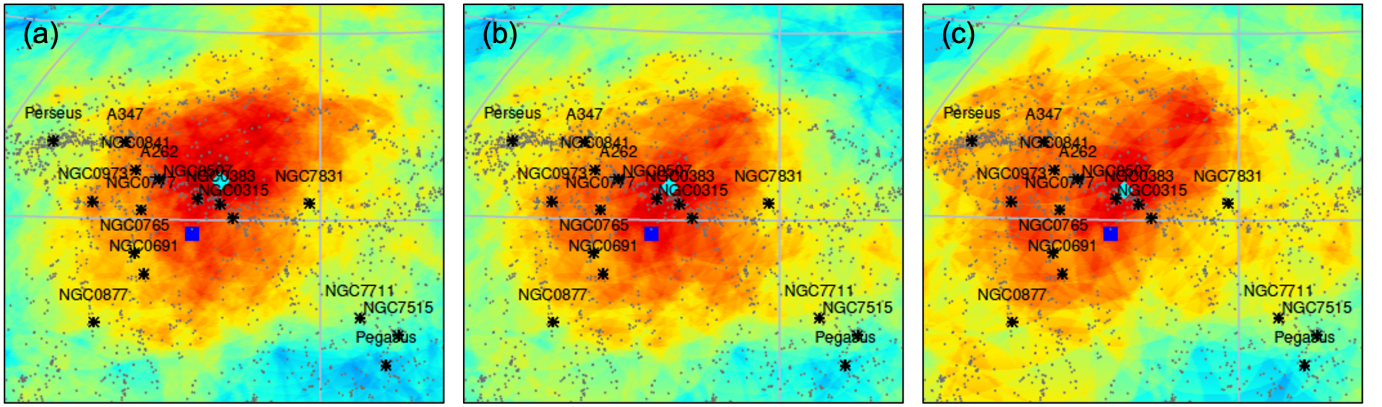
As an example, the Li-Ma significance map for the data set with  $E \geq 10^{19.5}$  eV is shown. The data do not show an excess at any of the locations of other major objects. All Li-Ma significances are less than  $1\sigma$ .

However, to see if it is likely that an excess at one of their locations could occur by chance, we repeated the MC calculation described in the previous paragraph, replacing the PPSC with all the major structures listed here including the PPSC. The chance probability of having an excess of equal or greater significance than that of the data on top of any of the five major structures are estimated to be  $3.1\sigma$ ,  $3.0\sigma$ , and  $2.9\sigma$  for  $E \geq 10^{19.4}$  eV,  $E \geq 10^{19.5}$  eV, and  $E \geq 10^{19.6}$  eV, respectively. These significances are sufficiently similar to that of the PPSC alone (about  $3.5\sigma$ ) that we conclude that random coincidences with the major objects of the local large-scale structure are unlikely.

We repeated the calculation using NASA/IPAC Extragalactic Database (NED 2021) centers of the major



**Figure 2.** Sky maps in equatorial coordinates. The Li-Ma significance analysis maps for the data set with  $E \geq 10^{19.5}$  eV. The results for the first 5-years of data are shown in the left and for the last 6-years of data on the right. The same color scheme as in Figure 1 is used. Both maps have a similar,  $\sim 3\sigma$ , excess in new region which indicates that it may be a steady state.



**Figure 3.** Expanded sky maps showing the new excesses of events overlaid with the major clusters and groups of galaxies of the Perseus-Pisces supercluster (PPSC). The color scheme is the same as that in Figure 1. The map is shown for three energy thresholds with minimum energy increasing from left to right: (a)  $E \geq 10^{19.4}$  eV, (b)  $E \geq 10^{19.5}$  eV, and (c)  $E \geq 10^{19.6}$  eV. The representative elements of the PPSC from reference (PPSC 2021) are indicated on the maps with black asterisks. Galaxies from the 2MASS Redshift Survey catalog (Huchra et al. 2012), with distances between 35 Mpc and 100 Mpc, are indicated with gray dots. These distances are similar to those of the PPSC representative elements. The positions of maximum excesses are marked with the cyan diamonds and the center of the PPSC is marked with the blue squares. It is seen that the excess is coincident with the overall distribution of the PPSC. The angular separations between the positions of the maximum excesses and the center of the PPSC are less than  $\sim 10^\circ$ .

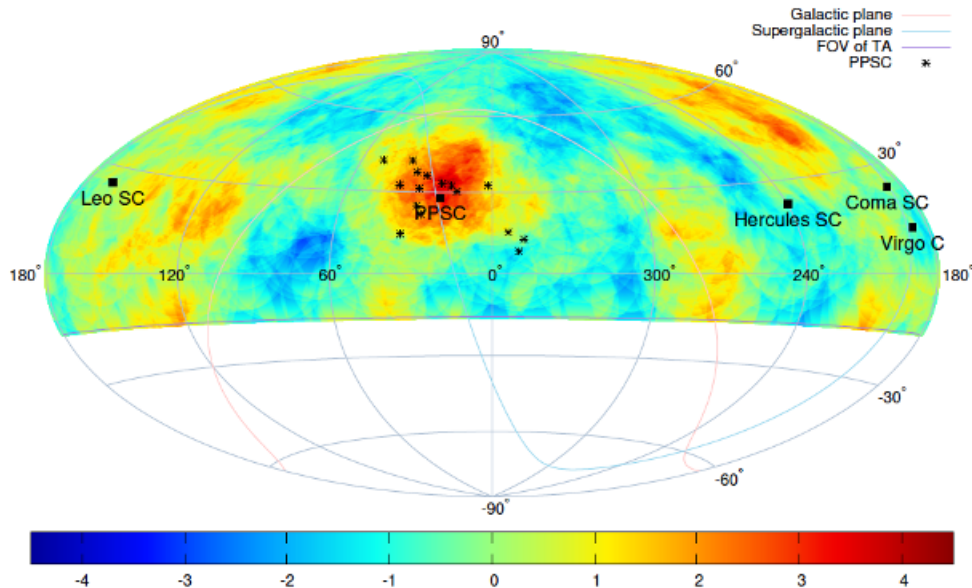
structures, and the significances were the same. The results are summarized in Table 1. Random coincidences between the data and the PPSC occur at the  $\sim 3.5\sigma$  level. This result indicates that it is likely there has a cosmic ray source in the Perseus-Pisces supercluster.

#### 4. SUMMARY

The TA Collaboration has observed a new excess of events in the arrival direction distribution. We found the excess over the isotropic background to have local significances of  $4.4\sigma$ ,  $4.2\sigma$ , and  $4.0\sigma$  for events of energy  $E \geq 10^{19.4}$  eV,  $E \geq 10^{19.5}$  eV, and  $E \geq 10^{19.6}$  eV, respectively, by using the Li-Ma method and a  $20^\circ$ -radius circle oversampling analysis. This excess overlaps with

the Perseus-Pisces supercluster which is a nearby element of the local large-scale structure of the universe and is the closest supercluster to us (other than the Virgo supercluster within which we reside).

When looking at the data overlaid with the PPSC, the excess is coincident with the overall distribution of the clusters and groups of galaxies within the Perseus-Pisces supercluster. To determine the probability that the data's  $4.0\sigma$ – $4.4\sigma$  significances could occur by chance close by the Perseus-Pisces supercluster, we generated isotropic Monte Carlo event sets with the same statistics as the data, thrown according to the acceptance of the TA surface detector. The chance probability of the



**Figure 4.** Sky map in equatorial coordinates. The Li-Ma significance analysis map for the data set with  $E \geq 10^{19.5}$  eV. The color scheme is the same as that in Figure 1. The representative clusters and groups of galaxies of the Perseus-Pisces supercluster (PPSC) are indicated by the black asterisks. The nearby major structures within the Telescope Array field of view—Virgo cluster (17 Mpc), PPSC (70 Mpc), Coma supercluster (90 Mpc), Leo supercluster (135 Mpc), and Hercules supercluster (135 Mpc)—are indicated by black squares. The data do not show an excess at any of the locations of other nearby major structures other than the PPSC. None of them have Li-Ma significances greater than  $1\sigma$ .

**Table 1.** Summary of the Monte-Carlo studies that estimate the chance probability of having an excess

Energy (eV)	Events	Criteria	Perseus-Pisces supercluster	Any of the Five Major structures
$E \geq 10^{19.4}$	864	$4.4\sigma$ & $8.6^\circ$	$3.6\sigma$	$3.1\sigma$
$E \geq 10^{19.5}$	558	$4.2\sigma$ & $7.4^\circ$	$3.6\sigma$	$3.0\sigma$
$E \geq 10^{19.6}$	335	$4.0\sigma$ & $6.8^\circ$	$3.4\sigma$	$2.9\sigma$

excess of events occurring coincident with the Perseus-Pisces supercluster has  $3.5\sigma$  significance.

We investigated whether there is another excess close to the locations of any of the nearby major structures similar to the Perseus-Pisces supercluster. None of them have Li-Ma significances larger than  $1\sigma$ . We repeated this process, testing the Monte Carlo event sets against the five nearby major astronomical structures. The significance of a random coincidence with any of them is estimated to be  $\sim 3\sigma$ .

The excess of events observed in the direction of the Perseus-Pisces supercluster indicates that a cosmic ray source likely exists in that supercluster. The supercluster contains many interesting astronomical objects, including active galaxies, starburst galaxies, and large-scale shocks, that may be UHECR sources. It is important to study these astronomical objects in the supercluster further, and to increase the statistical power of Northern Hemisphere cosmic ray studies.

The recent TA $\times 4$  project, which is the extension of the TA SD aperture by a factor of 4 and includes two new fluorescence detector stations which overlook the TA $\times 4$  SD array, is designed to study the highest energy cosmic rays (Abbasi et al. 2021b). As of 2021, more than half of the TA $\times 4$  SDs have been deployed and are operating successfully. Completing the construction of TA $\times 4$  and continuing to run TA will likely be an essential key to solving the problem of the origin of ultrahigh energy cosmic rays.

A table of events with energies above  $10^{19.4}$  eV is available in a machine-readable form in the online journal. It includes date and time, zenith angle, right ascension, and declination.

#### ACKNOWLEDGMENTS

The Telescope Array experiment is supported by the Japan Society for the Promotion of Science (JSPS) through Grants-in-Aid for Priority Area 431, for Specially Promoted Research JP21000002, for Scientific Re-

search (S) JP19104006, for Specially Promoted Research JP15H05693, for Scientific Research (S) JP15H05741, for Science Research (A) JP18H03705, for Young Scientists (A) JPH26707011, and for Fostering Joint International Research (B) JP19KK0074, by the joint research program of the Institute for Cosmic Ray Research (ICRR), The University of Tokyo; by the Pioneering Program of RIKEN for the Evolution of Matter in the Universe (r-EMU); by the U.S. National Science Foundation awards PHY-1404495, PHY-1404502, PHY-1607727, PHY-1712517, PHY-1806797, PHY-2012934, and PHY-2112904; by the National Research Foundation of Korea (2017K1A4A3015188, 2020R1A2C1008230, & 2020R1A2C2102800) ; by the Ministry of Science and Higher Education of the Russian Federation under the contract 075-15-2020-778, IISN project No. 4.4501.18, and Belgian Science Policy under IUAP VII/37 (ULB). This work was partially supported by the grants of The joint research program of the Institute for Space-Earth Environmental Research, Nagoya University and Inter-University Research Program of the Institute for Cosmic Ray Research of University of Tokyo. The foundations of Dr. Ezekiel R. and

Edna Wattis Dumke, Willard L. Eccles, and George S. and Dolores Doré Eccles all helped with generous donations. The State of Utah supported the project through its Economic Development Board, and the University of Utah through the Office of the Vice President for Research. The experimental site became available through the cooperation of the Utah School and Institutional Trust Lands Administration (SITLA), U.S. Bureau of Land Management (BLM), and the U.S. Air Force. We appreciate the assistance of the State of Utah and Fillmore offices of the BLM in crafting the Plan of Development for the site. Patrick A. Shea assisted the collaboration with valuable advice and supported the collaboration's efforts. The people and the officials of Millard County, Utah have been a source of steadfast and warm support for our work which we greatly appreciate. We are indebted to the Millard County Road Department for their efforts to maintain and clear the roads which get us to our sites. We gratefully acknowledge the contribution from the technical staffs of our home institutions. An allocation of computer time from the Center for High Performance Computing at the University of Utah is gratefully acknowledged.

## REFERENCES

- Aab, A., Abreu, P., Aglietta, M., et al. 2015, *Astrophysical Journal*, 804, 15, doi: [10.1088/0004-637x/804/1/15](https://doi.org/10.1088/0004-637x/804/1/15)
- . 2017, *Science*, 357, 1266, doi: [10.1126/science.aan4338](https://doi.org/10.1126/science.aan4338)
- Abbasi, R. U., Abe, M., Abu-Zayyad, T., et al. 2014, *Astrophysical Journal Letters*, 790, L21, doi: [10.1088/2041-8205/790/2/L21](https://doi.org/10.1088/2041-8205/790/2/L21)
- . 2018, *Astrophysical Journal*, 862, 91, doi: [10.3847/1538-4357/aac9c8](https://doi.org/10.3847/1538-4357/aac9c8)
- . 2021a, In preparation
- . 2021b, *Nuclear Instruments & Methods in Physics Research Section A: Accelerators, Spectrometers, Detectors and Associated Equipment*, 165726, doi: [10.1016/j.nima.2021.165726](https://doi.org/10.1016/j.nima.2021.165726)
- Abu-Zayyad, T., Aida, R., Allen, M., et al. 2012, *Nuclear Instruments and Methods in Physics Research Section a-Accelerators Spectrometers Detectors and Associated Equipment*, 689, 87, doi: [10.1016/j.nima.2012.05.079](https://doi.org/10.1016/j.nima.2012.05.079)
- . 2013, *Astrophysical Journal Letters*, 768, L1, doi: [10.1088/2041-8205/768/1/L1](https://doi.org/10.1088/2041-8205/768/1/L1)
- Batuski, D. J., & Burns, J. O. 1985, *Astrophysical Journal*, 299, 5, doi: [10.1086/163677](https://doi.org/10.1086/163677)
- Courtois, H. M., Pomaredé, D., Tully, R. B., Hoffman, Y., & Courtois, D. 2013, *Astronomical Journal*, 146, 69, doi: [10.1088/0004-6256/146/3/69](https://doi.org/10.1088/0004-6256/146/3/69)
- Haynes, M. P., & Giovanelli, R. 1986, *The Astrophysical Journal*, 306, L55, doi: [10.1086/184705](https://doi.org/10.1086/184705)
- He, H.-N., Kusenko, A., Nagataki, S., et al. 2016, *Phys. Rev. D*, 93, 043011, doi: [10.1103/PhysRevD.93.043011](https://doi.org/10.1103/PhysRevD.93.043011)
- Huchra, J. P., Macri, L. M., Masters, K. L., et al. 2012, *Astrophysical Journal Supplement Series*, 199, 22, doi: [10.1088/0067-0049/199/2/26](https://doi.org/10.1088/0067-0049/199/2/26)
- Kim, J., Ivanov, D., Kawata, K., et al. 2021, in 37th International Cosmic Ray Conference (ICRC2021) (Proceeding of Science), doi: [10.22323/1.395.0328](https://doi.org/10.22323/1.395.0328)
- Kim, J., Ryu, D., Kang, H., Kim, S., & Rey, S.-C. 2019, *Science Advances*, 5, eaau8227, doi: [10.1126/sciadv.aau8227](https://doi.org/10.1126/sciadv.aau8227)
- Li, T.-P., & Ma, Y.-Q. 1983, *Astrophysical Journal Letters*, 272, 317
- NED. 2021, NASA/IPAC Extragalactic Database. <http://ned.ipac.caltech.edu/>
- PPSC. 2021, The Perseus-Pisces Supercluster. <http://www.atlasoftheuniverse.com/superc/perpsc.html>
- Tokuno, H., Tameda, Y., Takeda, M., et al. 2012, *Nuclear Instruments & Methods in Physics Research Section a-Accelerators Spectrometers Detectors and Associated Equipment*, 676, 54, doi: [10.1016/j.nima.2012.02.044](https://doi.org/10.1016/j.nima.2012.02.044)